Search for $h \to aa \to \mu\mu\ \mu\mu$ or $\mu\mu\ \tau\tau$ with 3.7 fb^{-1} at DØ in Run II

The DØ Collaboration
URL http://www-d0.fnal.gov
(Dated: March 6, 2009)

The production of the lightest neutral CP-even Higgs boson (h) in the Next-to-Minimal Supersymmetric Standard Model (NMSSM) is searched for, where the h decays to a pair of lighter ($< \sim 10$ GeV) neutral pseudo-scalar Higgs bosons (a), using 3.7 fb^{-1} of $p\bar{p}$ collisions at $\sqrt{s} = 1960$ GeV recorded with the DØ detector at Fermilab. The a's are required to either both decay to $\mu^+\mu^-$ or one to $\mu^+\mu^-$ and the other to $\tau^+\tau^-$, where the tau's are identified as missing transverse energy. No signal is observed above backgrounds, and limits are set on $\sigma(p\bar{p} \to h + \mathrm{X}) \times \mathrm{BR}(h \to aa) \times \mathrm{BR}(a \to \mu^+\mu^-)^2$ or $\mathrm{BR}(a \to \mu^+\mu^-) \times \mathrm{BR}(a \to \tau^+\tau^-)$ as a function of M_a.

I. INTRODUCTION

In the Standard Model (SM), at least one Higgs boson is required in order to consistently give masses to the W and Z bosons. Extensions of the SM, such as supersymmetry, demand at least 3 neutral Higgs bosons [1]. Most naturally, the lightest neutral CP-even Higgs boson (h) in supersymmetric theories has a mass (M_h) near the Z boson mass (M_Z). Recent global electro-weak fits also prefer a Higgs boson lighter than 154 GeV at 95% C.L. [2]. But LEP has excluded an h boson decaying to $b\bar{b}$ with a mass below 114.4 GeV [3], resulting in fine-tuning being needed in the Minimal Supersymmetric extension of the SM (MSSM). Slightly richer models, such as the Next-to-Minimal Supersymmetric SM (NMSSM) [4] alleviate this fine-tuning, since the $h{\rightarrow}b\bar{b}$ branching ratio (BR) is greatly reduced because the h dominantly decays to a pair of lighter neutral pseudo-scalar Higgs bosons (a), giving a more complicated final state [5]. The most general LEP search irrespective of the Higgs decay only gives $M_h{>}82$ GeV[6], which is below M_Z.

In general, helicity suppression causes the a to decay to the heaviest pair of particles kinematically allowed. BR($a{\rightarrow}\mu^+\mu^-$) is predicted to be nearly 100% for $2M_\mu{<}M_a{<}{\sim}3M_\pi$ (~450 MeV) and then decreases with rising M_a from larger BR into hadronic states [7]. Evidence for a new particle consistent with an $a{\rightarrow}\mu\mu$ with M_a=214.3 MeV was seen by the HyperCP experiment [8]. Thus a dedicated search for $h{\rightarrow}aa$ with $a{\rightarrow}\mu\mu$ is well motivated [9]. Decays to charm are usually suppressed in the NMSSM, so they have been ignored.

If $M_a{>}2M_\tau$ (~3.6 GeV), it will decay primarily to a pair of taus, and the limits from LEP are still weak, ($M_h{>}86$ GeV) [10]. BR($a{\rightarrow}\mu^+\mu^-$) is suppressed by a factor of $(M_\mu^2/M_\tau^2)/(\sqrt{1-(2M_\tau/M_a)^2})$ (~ 1/270 at large M_a), so the 4μ channel would have very low rate. The direct search for the 4τ final-state is very challenging, due to the lack of an observable resonance and low e, μ p_T which complicates triggering [11]. The $2\mu2\tau$ final-state however contains a resonance from $a{\rightarrow}\mu^+\mu^-$, high p_T muons useful for triggering, and missing transverse energy ($\not{E}_T$) from the $a{\rightarrow}\tau^+\tau^-$ decay containing neutrinos.

In this note, a search for h production, followed by $h{\rightarrow}aa$ with either both a's decaying to $\mu^+\mu^-$ or one decaying to $\mu^+\mu^-$ and the other to $\tau^+\tau^-$ is presented. Data from Run II of the Fermilab Tevatron collider recorded with the DØ detector [12] is used, corresponding to an integrated luminosity of about 3.7 fb^{-1}. The signal signature is either two pairs of very collinear muons (due to the low a mass), or one pair of collinear muons and large $\not{E}_T$ (from $a{\rightarrow}\tau^+\tau^-$) opposite the muon pair. The main backgrounds are QCD, where jets create muons in the decay of particles in flight (π,K) or from heavy-flavor decays and other sources (η,ϕ,J/ψ, etc.), and Z/$\gamma^\star{\rightarrow}\mu\mu$ + jets.

II. SIMULATION

The pythia [13] event generator was used to simulate signals, then passed through GEANT3 [14] DØ detector simulation, overlaid with zero-bias events from data to simulate effects from additional $p\bar{p}$ interactions, and reconstructed. The $gg{\rightarrow}h{\rightarrow}aa$ process was generated and each a was either forced to decay to a pair of muons (for the 4μ channel) or allowed to decay to gluons, electrons, muons, or taus. Approximately 10000 events were generated for various M_h and M_a.

III. EVENT SELECTION

Events are required to have at least two muons reconstructed in the muon system and matched to central tracks from the inner tracking system with $p_T{>}10$ GeV. No requirement is made that the muons be opposite electric charge sign. No specific trigger requirements were made, in order to retain the highest possible efficiency for signal. Comparisons between the data and Z$\rightarrow\mu\mu$ simulation after appropriate corrections show no significant kinematic biases, and the NNLO Z cross section agrees within errors with that from the luminosity system. Trigger efficiency is found to be higher than 90% for events passing offline selection.

IV. THE 4μ CHANNEL

For the 4μ channel, two of these muons must have $\Delta R(\mu,\mu) > 1$ and invariant mass greater than 15 GeV. Only one muon is required to be reconstructed from each pair of collinear muons, since the muon system has insufficient granularity to reliably reconstruct the two nearby muons. To identify the collinear muon signature, a "companion" track is identified with $p_T{>}4$ GeV and smallest ΔR from each muon, within $\Delta R{<}1$. An event display of a simulated 4μ event is shown in Figure 4.
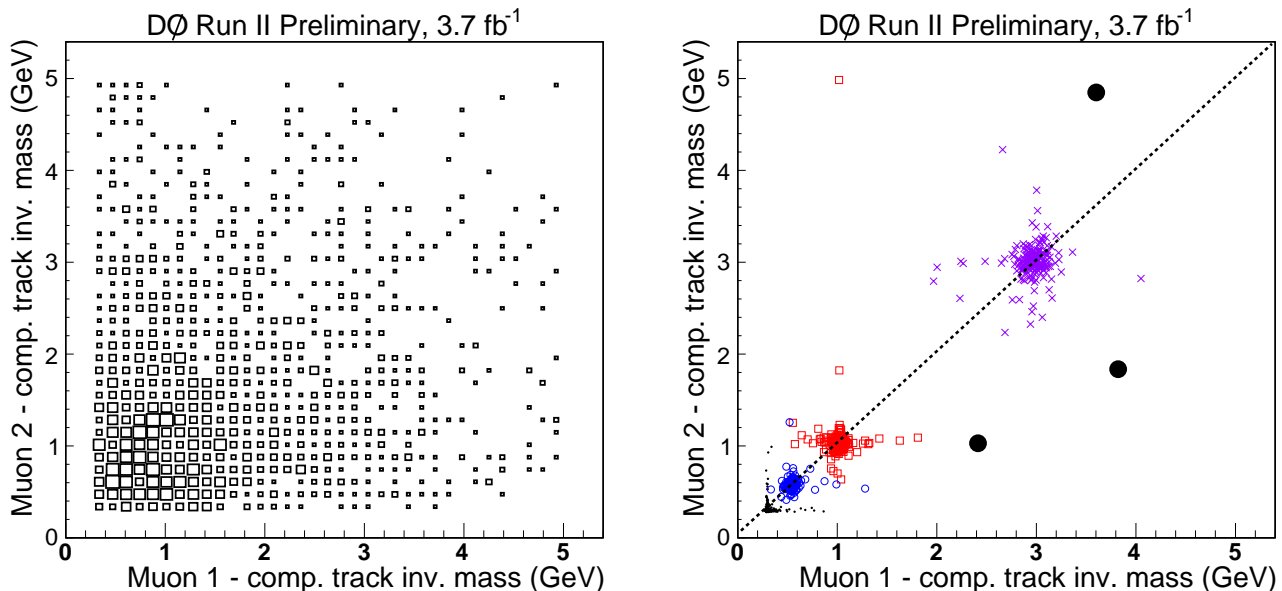
FIG. 1: The mass of the muon and the companion track for the leading vs. second-leading p_T muons in the QCD sample (left). The mass of the muon and the companion track for the leading vs. second-leading p_T muons remaining after isolation is applied to both muons for data (solid big black dots), and various signal masses generated: 0.2143 GeV (small black dots), 0.5 GeV (open blue circles), 1 GeV (open red squares), and 3 GeV (purple crosses) (right).

Muon calorimeter isolation is typically defined as the sum of the transverse energies of all calorimeter cells in a hollow cone around the muon from $0.1<\Delta R<0.4$. Due to the unusual signal topology which has a second collinear muon that could often leave energy within the isolation cone of the other muon, a modified definition is used, called "muon pair isolation". The sum of calorimeter cell energy is calculated within $\Delta R>0.1$ and $\Delta R<0.4$ of *either* the muon track or the companion track. Both muons are required to have muon calorimeter pair isolation less than 1 GeV. Many signal events have a single extra track in a track isolation cone of $\Delta R<0.5$ around each muon, from the collinear muon. But there is often another track also in the cone, perhaps from the underlying event. We accept events with ≤ 3 tracks, including the muon track itself, with $p_T> 0.5$ GeV in the track isolation cone of each muon. Approximately 20% of signal events pass all selections, with weak dependence on M_h and M_a.

To study the probability for a jet to produce a muon passing our cuts, we look at a control sample greatly enhanced in QCD by removing the calorimeter isolation cuts on the muons. Just 2.5% of jets have pair calorimeter isolation <1 GeV, even after requiring ≤ 3 tracks in the track isolation cone of each muon, and reasonable pair calorimeter isolation (<10 GeV) for the other muon. Given 1890 events in the QCD sample, we would expect about 1.2±0.4 events to have both muons pass calorimeter isolation. The distribution of the events in the QCD sample for one muon-track mass vs. the other is shown in Figure 1 (left). Background is also observed from $Z/\gamma^\star\to\mu\mu$ events where additional, possibly fake, companion tracks are reconstructed. Studying the di-muon mass distributions in the isolated data when zero or one of the muons are required to have companion tracks gives an estimate of 0.25±0.03 events from this source. The background from other sources such as $t\bar{t}$, di-boson, or W+jets production is found to be negligible in this channel.

After calorimeter isolation is applied to both muons, there are three events observed in data, see Figure 1 (right), consistent with the total background of 1.5±0.5 events. No clustering of the isolated data events is found in muon-track mass, compared to strong peaking in the mass distribution for signal. Also, none have a third muon identified, as opposed to about 50% of the simulated signal events.

The uncertainty on the signal acceptance is dominated by the ability of the MC to properly simulate the detection of the companion track, particularly in the case where the two muons are very collinear. We know from studies of $Z\to\mu\mu$ events that the relative tracking efficiency for isolated high p_T tracks in data is within 10% of that in the simulation. For smaller opening angles, we compare K_s decays in data and simulation as a function of the opening angle of the two pion tracks. Stable behavior is seen over most of the ΔR range within 20%. Below $\Delta R<0.02$, consistency can only be confirmed at the 50% level. Muon ID and trigger efficiency are well-constrained by the agreement between $Z\to\mu\mu$ MC and data, to better than 5%, for most of the $\Delta R(\mu,\mu)$ range. Below $\Delta R(\mu,\mu)<0.1$, there is the possibility that the two muons will overlap in the muon system and interfere with each other's proper reconstruction in the data and/or simulation. By studying the effect of adding additional noise hits on the muon reconstruction, we have

TABLE I: The 2D 2σ window position and width, efficiency for signal within the window, and number of events expected from background, observed in data, and the expected and observed limits on $\sigma(p\bar{p}{\rightarrow}h{+}\mathrm{X}){\rightarrow}aa{\rightarrow}4\mu$, for each M_a studied, assuming $M_h{=}100$ GeV. The background uncertainties shown are the statistical only.

M_a (GeV)	2D Window (GeV)	Eff.	N bgnd. total	N data	[exp.] obs. (fb)
0.2143	0.295±.016	17%	0.001±0.001	0	[12.0] 12.0
0.3	0.37±.06	15%	0.005±0.002	0	[10.5] 10.5
0.5	0.57±.08	11%	0.011±0.004	0	[9.5] 9.5
1	1.02±.12	12%	0.023±0.005	0	[9.3] 9.3
3	3.01±.20	11%	0.005±0.002	0	[9.5] 9.5

confirmed that muon efficiency can be affected by up to 10%. Also, the di-muon trigger may lose efficiency due to degraded momentum resolution from pattern recognition errors, leading to an additional trigger efficiency uncertainty of 20%. Background uncertainty is dominated by the statistical uncertainty of the QCD-enhanced data sample and is within 50%. Luminosity uncertainty is 6.1%.

The signal dimuon mass peak is fit to a Gaussian, and the number of events with muon - companion track masses of *both* muons within a $\pm 2\sigma$ window around the fit's mean are counted, for data, signal, and background. Thus a square 2D window is defined in the muon - companion track pair 1 mass vs. muon - companion track pair 2 mass plane. Table I shows the 2D window size and efficiency from signal, number of events expected from background, number of events observed in data, and the expected and observed limits, set using a Bayesian technique [15], on the cross section times BR of $h{\rightarrow}aa{\rightarrow}4\mu$, for each M_a studied, assuming $M_h{=}100$ GeV. Limits vary slightly with M_h, decreasing by $\sim$10% when M_h increases from 80 to 150 GeV.

V. THE $2\mu 2\tau$ CHANNEL

For the $2\mu 2\tau$ channel, a muon pair is required in each event, defined as the highest p_T muons that have $p_T{>}10$ GeV and $\Delta R(\mu\mu){<}0.5$ and $\mathrm{M}(\mu\mu){<}20$ GeV. This is the "pre-selection" stage (see Table II). Next, the sum of the p_T of the two muons is required to be greater than 35 GeV, to reduce $\gamma^{\star}{\rightarrow}\mu\mu$ background. The same muon calorimeter pair and track isolation cuts are applied as for the 4μ channel. This is the "isolated" stage. An event display of a simulated $2\mu 2\tau$ event is shown in Figure 5.

Traditional τ-ID is severely degraded and complicated by the topology of the two overlapping τ's. Instead, we will be requiring significant $\not{E}_T$ ($>$25 GeV) from the collinear τ decays to τ neutrinos and often additional leptonic τ decays to muons and/or electrons. The $\not{E}_T$ is corrected for the transverse momentum of the muons. To ensure that this correction is as accurate as possible, additional muon criteria are applied. The muons' tracks in the inner tracker are required to have fits to their hits with $\chi^2/ndof{<}4$, transverse impact parameter from the primary vertex less than 0.01 cm, and at least three silicon hits. The match between the muon system track and the track in the inner tracker must have $\chi^2{<}40$, and the muon system track must have $p_T{>}8$ GeV. Hits are required for both muons in all three layers of the muon system. Also, less than 10 GeV of transverse energy is allowed within $\Delta R{<}0.1$ of either muon, to prevent the case where muons have large showers in the calorimeter, since these lead to inaccurate muon correction of the $\not{E}_T$. Finally, the leading muon p_T must be less than 80 GeV, to prevent against grossly mis-measured muons. To improve the $\not{E}_T$ measurement in the calorimeter, the number of jets reconstructed with the DØ Run II cone algorithm [16] of cone radius 0.5 with $p_T{>}15$ GeV (corrected for jet energy scale) must not be more than two. Events with $\not{E}_T{>}80$ GeV are also rejected, since signal is not expected with such large $\not{E}_T$. This is the "refined" stage. In addition to requiring $\not{E}_T{>}25$ GeV the azimuthal angle between the muon pair (calculated as the p_T weighted sum of the two muons' ϕ) and $\not{E}_T$ ϕ is required to be larger than 2.5, i.e. back-to-back with the muon pair. This is the final, "$\not{E}_T$" stage. An event from data passing all these selections is shown in Figure 6.

The shape of the estimated background is taken from the data passing all selections except with $\not{E}_T{<}25$ GeV. This background shape is then normalized to the data passing all selections, including $\not{E}_T{>}25$ $\not{E}_T$, but excluding data events within each 2σ dimuon mass window for each M_a (see below). The resulting background shape is shown in Figure 2, along with the high $\not{E}_T$ data and various signals (scaled by 4 for visibility). Additional background from di-boson, $t\bar{t}$, and W+jets production were estimated using pythia samples run through full GEANT simulation and reconstruction and found to be smaller than 10% of the background from QCD and $\gamma^{\star}$.

Signal acceptance uncertainty for the $2\mu 2\tau$ channel is dominated by the ability of the simulation to model the efficiency of the non-standard "refining" muon cuts. Studies of the muon quantities used, comparing data and MC muons in the Z mass peak show agreement within 20%. Signal trigger efficiency is understood to within 10% by
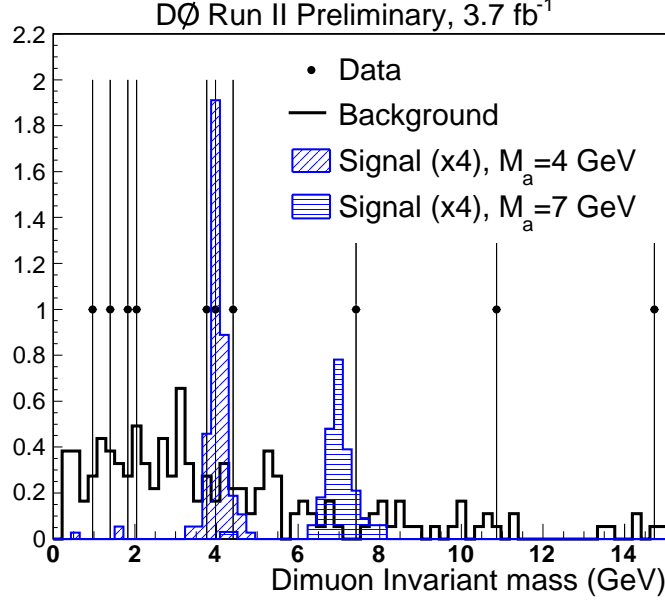
FIG. 2: The di-muon invariant mass for events passing all selections in data (points), background (line), and $2\mu2\tau$ signal for M_a=4 and 7 GeV scaled by 4 (shaded). For the signals, a $p\bar{p}{\rightarrow}h{+}X$ cross section of 1 pb was assumed, BR($h{\rightarrow}aa$)=1, and a decays as given by pythia (with no charm decays).

TABLE II: Selection efficiencies and limits for the $2\mu2\tau$ analysis, for M_h=100 GeV and various M_a, assuming the a BR's given by pythia (with no charm decays). The number of generated events, having at least 2 muons with p_T>10 GeV at the generator level, at least 2 reconstructed muons passing pre-selection criteria with ΔR<0.5 and M(μ,μ)<20 GeV, and at "isolated", "refined", and final "$\not{E}_T$" stages. The 2σ window size and number of events within the window (and overall efficiency) follows. Next are shown the overall efficiency for signal, number of events expected from background, observed in data, and the expected and observed limits on $\sigma(p\bar{p}{\rightarrow}h{+}X)\times$BR($h{\rightarrow}aa$). Also, "model-independent" expected and observed limits on $\sigma(p\bar{p}{\rightarrow}h{+}X)\times$ BR($h{\rightarrow}aa$) $\times$ 2 $\times$ BR($a{\rightarrow}\mu^+\mu^-$)$\times$BR($a{\rightarrow}\tau^+\tau^-$) are given. The quoted uncertainties are statistical only.

Sample	N gen.	N 2μ	N pre.	N iso.	N ref.	N $\not{E}_T$	Win. (GeV)	N win. (eff.)	N bgnd.	N data	[exp.] obs. (fb)	$\sigma\times$BR [exp.] obs. (fb)
Data	-	-	76773	2199	678	10	-	-	-	-	-	-
M_a=4 GeV	550000	7700	2208	1012	483	140	±0.4	124 (.023%)	0.6±0.2	3	[5000] 8600	[46] 80
M_a=7 GeV	492500	5910	1174	506	250	79	±0.6	68 (.014%)	0.3±0.1	1	[5900] 8800	[36] 56

comparing the J/ψ and Z yields. Background uncertainty is dominated by the statistical uncertainty of the data sample passing all selections but with $\not{E}_T$<25 GeV, and is within 30%. Alternate fits of the background shape from low $\not{E}_T$ data with various selections modified the background estimates by up to 10%. Luminosity uncertainty is again 6.1%.

The signal dimuon mass peak is fit to a Gaussian, and the number of events with dimuon mass within a $\pm2\sigma$ window around the fit's mean are counted, for data, signal, and background (see Table II). The expected and observed limits on the cross section times BR of the $h{\rightarrow}aa$ process for each M_a studied are shown, assuming the a BR's given by pythia (with no charm decays). Limits are derived for additional M_a by interpolating the signal efficiencies and window sizes, see Figure 3. Since the a BR's are model-dependent, we also derive a result which factors out the BR's taken from pythia (for $a{\rightarrow}\mu\mu,\tau\tau$: .0060,.78 for M_a=4 GeV and .0036,.87 for 7 GeV). We also study the change in limits vs. M_h, see Tab. III.

VI. CONCLUSIONS

The first search for Higgs production in the NMSSM decaying into a bosons at a high-energy hadron collider has been presented, in the 4μ and $2\mu2\tau$ channels. At low M_a, <$2M_\tau$, the 4μ channel is relevant, and limits on $\sigma(p\bar{p}{\rightarrow}h{+}X)\times$
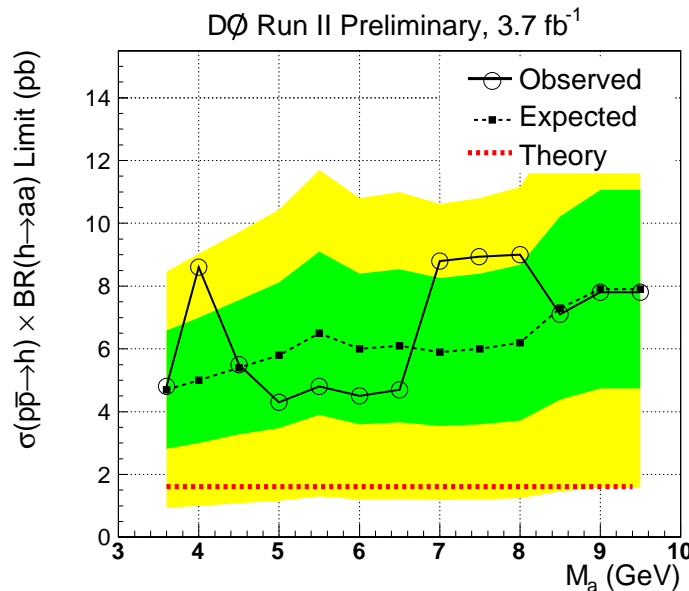
FIG. 3: The expected (small dots) and observed (open circles) limits and ± 1 and 2σ expected limit bands (shaded green, yellow) for $\sigma(p\bar{p}\to h+X)\times BR(h\to aa)$, for each M_a studied and M_h=100 GeV. The a BR's given by pythia are assumed, with no charm decays. The SM Higgs cross section is shown by the dashed band, for M_h=100 GeV.

TABLE III: Selection efficiencies for the $2\mu2\tau$ analysis and the expected and observed limits on $\sigma(p\bar{p}\to h+X)\times BR(h\to aa)$, for M_a=4 GeV and various M_h, assuming the a BR's given by pythia (with no charm decays). Also shown is the cross section for Higgs boson production in the SM, for comparison.

M_h (GeV)	Eff.	[exp.] obs. (fb)	σSM (fb)
87	.014%	[8200] 14000	2100
100	.023%	[5000] 8600	1650
150	.041%	[2800] 4500	525

BR($h\to aa$) $\times$ BR($a\to\mu^+\mu^-$)^2 of about 10 fb have been set. Assuming a Higgs cross section of 1000 fb [17], corresponding to the SM and $M_h\sim$120 GeV, the BR($a\to\mu\mu$) must therefore be less than about 10% to avoid detection, assuming a large BR($h\to aa$). The predicted BR($a\to\mu\mu$) is driven at low M_a by competition between decays to $\mu\mu$ and to gluons [7] and is larger than 10% for all $M_a<2M_c$. Depending on the BR of a to charm, which is model-dependent and typically suppressed in the NMSSM, BR($a\to\mu\mu$) could remain above 10% until $2M_\tau$. For $M_a>2M_\tau$, the limits set by the current analysis are still a factor of $\sim$4 larger than the expected Higgs production. Approximately 40 fb^{-1} of data would be required to be sensitive to the expected signal level.

[1] J. R. Ellis, D. Nanopoulos, K. A. Olive and Y. Santoso, Phys. Lett. B **633**, 583 (2006).

[2] The LEP Electroweak Working Group, arXiv:0712.0929 [hep-ex] (2007) and update from July 2008 on http://lepewwg.web.cern.ch/LEPEWWG/.

[3] R. Barate *et al.*, Phys. Lett. B **565**, 61 (2003).

[4] U. Ellwanger, M. Rausch de Traubenberg and C. A. Savoy, Nucl. Phys. B **492**, 21 (1997).

[5] S. Chang, R. Dermisek, J. F. Gunion and N. Weiner, arXiv:0801.4554 [hep-ph] (2008).

[6] OPAL, G. Abbiendi *et al.*, Eur. Phys. J. C**27**, 311 (2003).

[7] K. Cheung, J. Song, P. Tseng and Q. S. Yan, arXiv:0806.4411 [hep-ph] (2008).

[8] H. Park *et al.* [HyperCP Collaboration], Phys. Rev. Lett. **94**, 021801 (2005).

[9] S. h. Zhu, arXiv:hep-ph/0611270 (2006).

[10] ALEPH, S. Schael *et al.*, Eur. Phys. J. C**47**, 547 (2006).

[11] P. W. Graham, A. Pierce and J. G. Wacker, arXiv:hep-ph/0605162 (2006).

[12] DØ Collaboration, V. Abazov *et al.*, Nucl. Instrum. Methods Phys. Res. A. **565**, 463 (2006).

[13] T. Sjöstrand *et al.*, Comp. Phys. Comm. **135**, 238 (2001).

[14] R. Brun and F. Carminati, CERN Program Library Long Writeup W5013, 1993 (unpublished).

[15] I. Bertram *et al.*, FERMILAB-TM-2104, Apr 2000.

[16] G. C. Blazey *et al.*, in *Proceedings of the Workshop: "QCD and Weak Boson Physics in Run II,"* edited by U. Baur, R. K. Ellis, and D. Zeppenfeld, (Fermilab, Batavia, IL, 2000) p. 47.
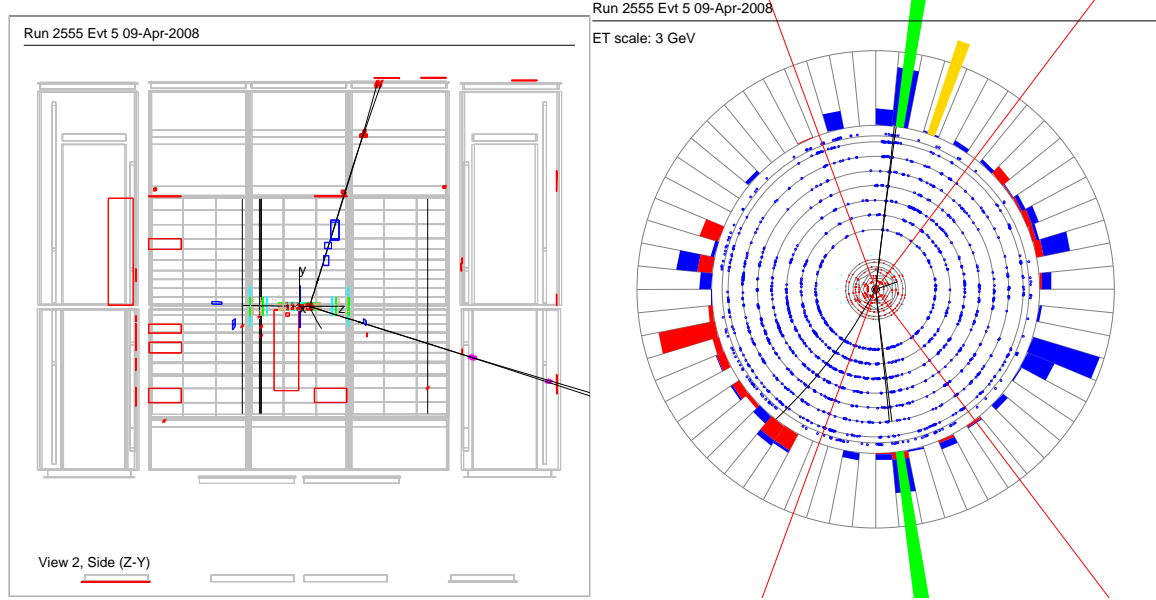
[17] T. Hahn *et al.*, arXiv:hep-ph/0607308 (2006).

Run 2555 Evt 5 09-Apr-2008

Run 2555 Evt 5 09-Apr-2008

ET scale: 3 GeV

View 2, Side (Z-Y)

FIG. 4: A simulated $h{\to}aa{\to}4\mu$ event with M_h=100 GeV and M_a=214.3 MeV.

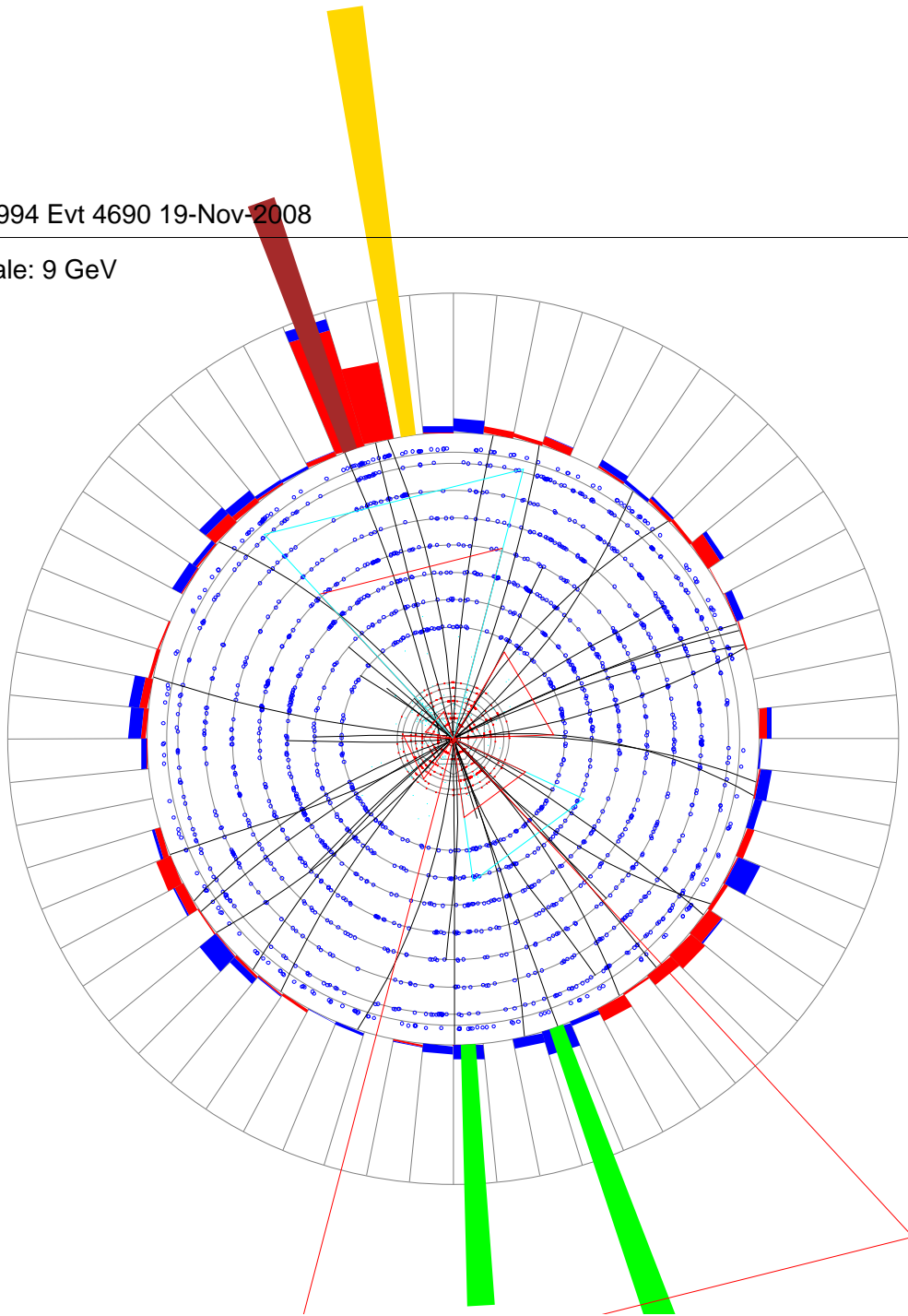Run 2994 Evt 4690 19-Nov-2008

ET scale: 9 GeV

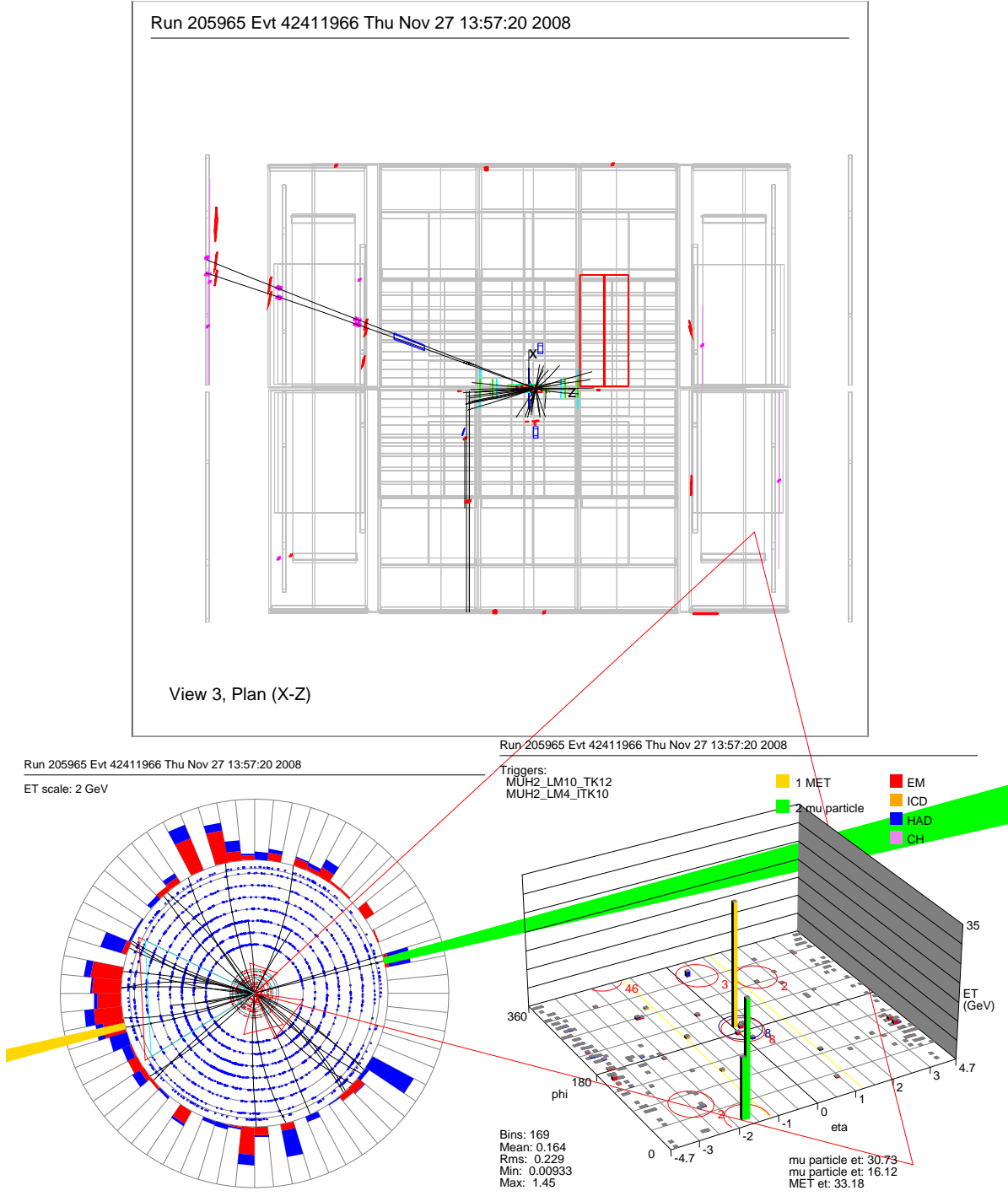FIG. 5: XY view of a simulated $2\mu2\tau$ signal event with M_a=7 GeV.

FIG. 6: Views of an event in data passing all the final "$\not{E}_T$" selections for the $2\mu2\tau$ channel.